

BEAM-BASED MEASUREMENT OF ID TAPER IMPEDANCE AT DIAMOND

V. Smaluk[#], R. Fielder, G. Rehm, Diamond Light Source, Oxfordshire, UK
R. Bartolini, Diamond Light Source, Oxfordshire, UK and JAI, Oxford, UK

Abstract

New insertion devices (IDs) are being designed now for a Diamond upgrade. For in-vacuum undulators, one of the important topics of the design is the coupling impedance of the ID vacuum chamber. To get complete and reliable information of the impedance, numerical simulation and beam-based measurement have been performed. The impedance of an existing ID taper geometrically similar to the new one has been measured using the orbit bump method. It turns out that in spite of the small magnitude (few μm) of orbit distortion to be observed in this case, the BPM resolution is sufficient for this measurement. The measurement results in comparison with simulation data are discussed in this paper.

INTRODUCTION

Current upgrade plan for the Diamond Light Source includes introducing additional insertion device (ID) straights to increase the capacity of the facility. It is proposed to convert some of the DBA lattice cells into a double-DBA, with a new ID straight between the two achromats [1]. The new lattice allows the introduction of a 2-m long in-vacuum ID with 5 mm gap without impacting the limiting aperture of the existing ring and with negligible impact on emittance and energy spread.

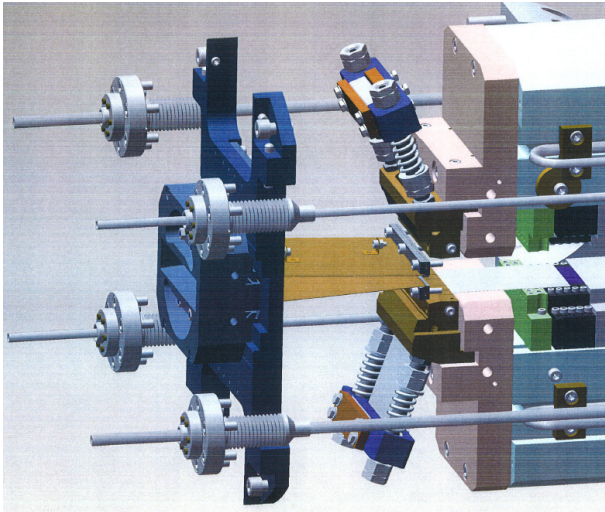


Figure 1: Layout of the tapered transition.

A standard U21 in-vacuum ID was assumed for the new beamline, although a CPMU is also under consideration. For the in-vacuum undulators, one of the important issues of design is the coupling impedance of the ID vacuum

chamber. The chamber includes flat tapered transitions, vertical aperture of which can be changed from 5 mm (ID closed) up to 30 mm (ID open), see Fig. 1. The entry and exit vertical aperture of the ID vacuum chamber is 18.4 mm, the length of taper is 108.5 mm, and the width of parallel copper plates forming the transition is 84 mm.

A possibility of decreasing the taper length has been studied because of the limited longitudinal space in the new ID section. To get complete and reliable information of the coupling impedance, numerical simulation and beam-based measurement have been performed.

CST SIMULATION

Both longitudinal and transverse wake fields and impedances of the new ID section vacuum chamber have been calculated using 3D simulation code CST Particle Studio [2]. Transverse wake fields have been simulated for a range of the ID gap values. To reduce the computing time, a model with simplified geometry was used, see Fig. 2. The length of the central part is 20 mm in the model, whereas the real undulator is 2480 mm long, the entrance and exit apertures are $84 \times 18.4 \text{ mm}^2$, and the vertical size of the central part varies from 4 mm up to 30 mm with 2 mm step.

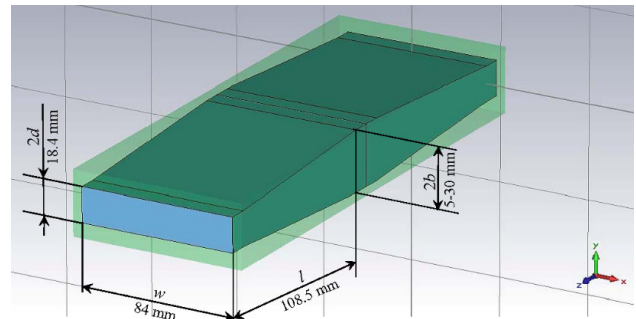


Figure 2: CST model.

To compare with the measurement results, the vertical kick factor k_{\perp} was calculated using CST Particle Studio simulation data. The kick factor k_{\perp} is a function of the transverse dipole impedance $Z_{\perp}(\omega)$ and the bunch power spectrum $h(\omega) = \lambda(\omega)\lambda^*(\omega)$, or, in time domain, a function of the wake potential $V_{\perp}(t)$ and beam linear density $\lambda(t)$:

$$k_{\perp} = \frac{1}{\pi} \int_0^{\infty} \text{Im} Z_{\perp}(\omega) h(\omega) d\omega = \int_{-\infty}^{\infty} V_{\perp}(t) \lambda(t) dt, \quad (1)$$

where $\lambda(\omega)$ is the Fourier transform of $\lambda(t)$.

[#] victor.smalyuk@diamond.ac.uk

Figure 3 shows an example of simulated vertical wake potential (a) and impedance (b), beam linear density is also shown.

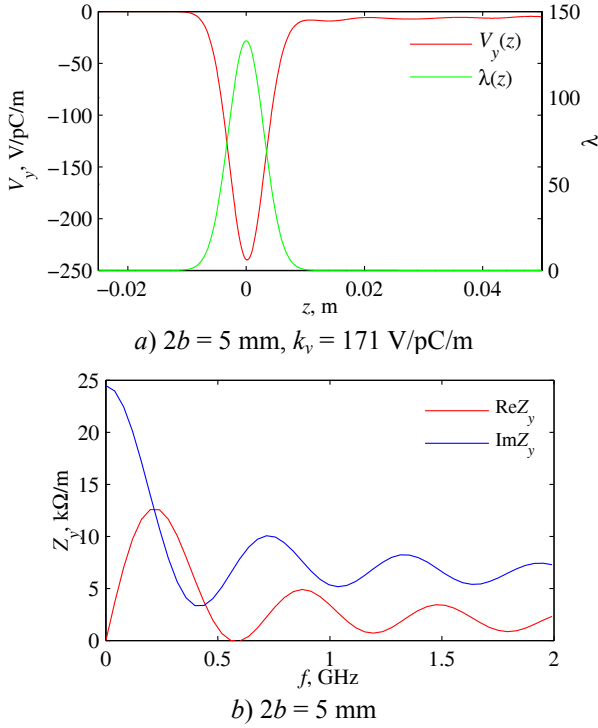


Figure 3: Wake potential (a) and impedance (b) calculated by CST Particle Studio.

MEASUREMENT TECHNIQUE

To estimate impedance of the new ID taper, the kick factor of an existing ID taper geometrically similar to the new one has been measured using the orbit bump method. The measurement technique has been developed and realised first at Budker Institute of Nuclear Physics [3,4]. Later, this technique was used for measurements of the narrow-gap ID chambers impedance at APS [5] and impedance of a movable beam scraper at ELETTRA [6].

The method is based on the fact that an off-axis beam passing through the vacuum chamber section with a non-zero transverse impedance is deflected by the wake-fields. If a bunched beam is displaced from the equilibrium orbit at the location of the transverse impedance, the beam-impedance interaction results in a kick of the beam transverse momentum $\Delta y'$ proportional to the beam displacement y_0 at the impedance location:

$$\Delta y' = \frac{q}{E/e} k_{\perp} y_0, \quad (2)$$

where q is the bunch charge, E is its energy, and k_{\perp} is the kick factor (1).

Thus, if an orbit bump is created at the impedance location s_0 and two orbits are measured with different

beam intensity, the orbit deviation caused by the beam-impedance interaction is:

$$\Delta y(s) = \frac{\Delta q}{E/e} k_{\perp} y_0 \frac{\sqrt{\beta(s_0)\beta(s)}}{2 \sin \pi \nu} \times \cos(|\mu(s) - \mu(s_0)| - \pi \nu), \quad (3)$$

where Δq is the bunch charge variation, ν is the betatron tune, β is the beta function, and μ is the betatron phase advance. This wave-like orbit deviation can be measured using beam position monitors (BPMs), and the wave amplitude gives the information about the reactive part of dipole transverse impedance at the bump location.

To reduce the systematic error caused by intensity-dependent behaviour of the BPM electronics, this error is also measured and then subtracted. First of all, after the initial global correction of orbit to zero, two reference orbits y_{01} and y_{02} are measured at the high and low values of beam current. Then, after creating the orbit bump, two orbits y_1 and y_2 are measured again at the same beam current values. In the four-orbit combination $\Delta y = (y_2 - y_1) - (y_{02} - y_{01})$, the systematic error is eliminated, as well as the bump itself.

Relative accuracy of the kick factor measurement depends on the BPM resolution δy_{BPM} as

$$\frac{\delta k_{\perp}}{k_{\perp}} = 2 \frac{\delta y_{\text{BPM}}}{\Delta y} \frac{1}{\sqrt{N}}, \quad (4)$$

where $N \gg 1$ is the number of BPMs. In spite of the small magnitude (few μm) of orbit deviation to be observed, the resolution of Diamond BPMs is sufficient for this measurement.

MEASUREMENT RESULTS

The vertical kick factor of ID16 has been measured for 7 values of the ID gap height. Note that a single-bunch effect was measured and the orbit deviation (3) is proportional to the single bunch charge variation. But due to the limitation of a single-bunch current in the Diamond storage ring, the measurements were carried out with a special beam filling pattern: 5 or 10 equally-spaced bunches. This was done to improve the BPM performance, because the BPM sensitivity is proportional to the average beam current. We assume that the bunch-to-bunch distance was large enough to let the short-range wake fields disappear, and there was no bunch-to-bunch interaction.

Figure 4 and Fig. 5 show the orbit deviation (3) measured with the same gap height of 5 mm (ID closed), but the first measurement has been performed with the bunch charge difference $\Delta q = 1.4$ nC and the bump height $y_0 = 1.0$ mm, whereas for the second measurement $\Delta q = 2.5$ nC and $y_0 = 1.5$ mm. As one can see, the orbit wave amplitude increases proportionally.

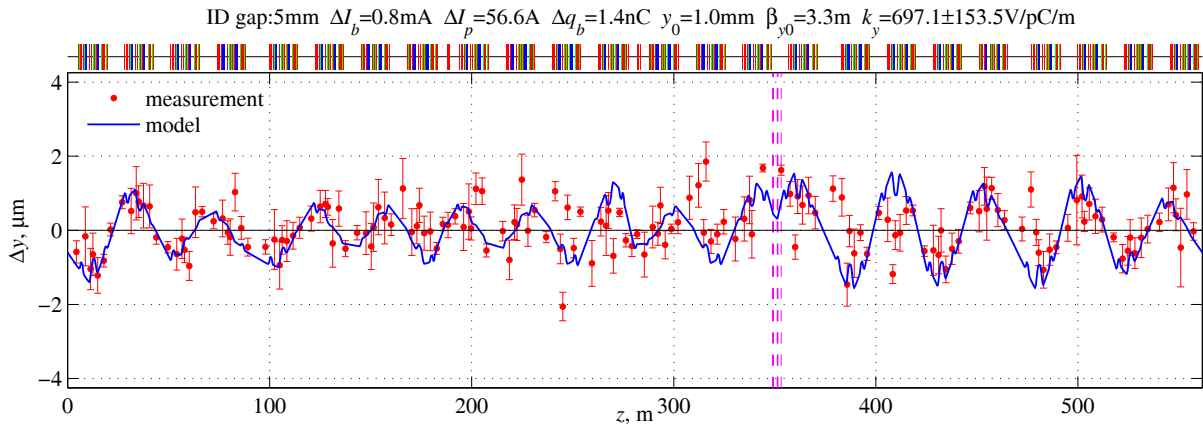


Figure 4: Orbit deviation: $\Delta q = 1.4 \text{ nC}$, $y_0 = 1.0 \text{ mm}$.

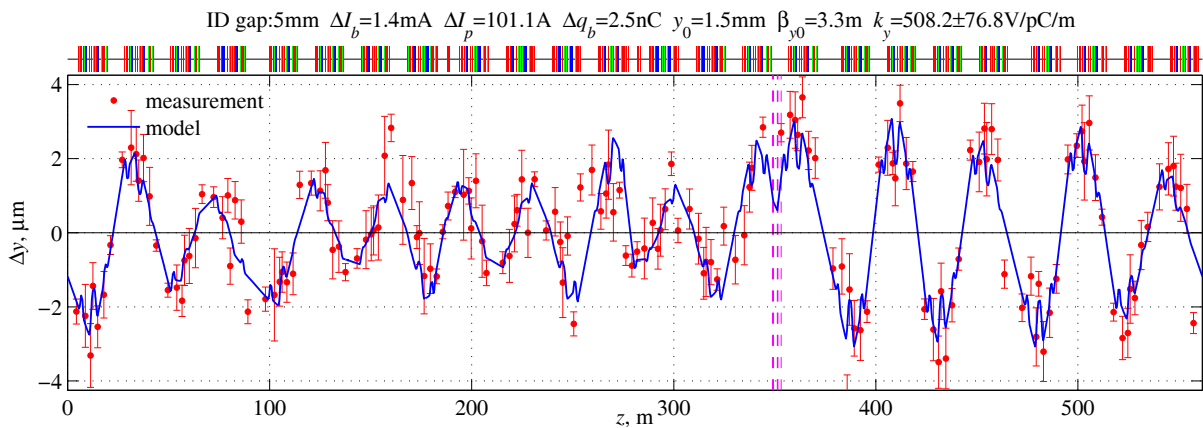


Figure 5: Orbit deviation: $\Delta q = 2.5 \text{ nC}$, $y_0 = 1.5 \text{ mm}$.

In these graphs, the red dots represent average values of 10 consecutive measurements of beam position and the error bars – standard deviations. The solid line is the model orbit deviation (3) fitting the measured data with k_{\perp} as a fit parameter. Note that the pure BPM noise resulting in uncorrelated beam position uncertainty is not expected to be that large. So we can suspect that there were real orbit fluctuations (correlated motion due to a single or several unstable correctors), which might have some impact on the error estimate. As a result, the error bars in Fig. 4 and Fig. 5 represent the integral error of the orbit measurement including both BPM noise and beam position fluctuations.

Note that formula (3) is derived for a short bump, with the beta function $\beta(s_0)$ and betatron phase advance $\mu(s_0)$ assumed constant through the bump length. As for the real measurements, the bump length is a couple of meters, and the beta function and betatron phase has been taken averaged over the bump length. Thus the measured orbit deviation represents effects of all impedances located within the bump.

The measurement results are summarized in Fig. 6. There are values of the vertical kick factor k_y calculated using the measured data in comparison with the CST Particle Studio simulation data. Since the simulation has

been carried out for the simplified ID taper and the contribution of the other environment was not taken into account, an offset has been added to the simulation data for better fit of the measured kick factor. Actually, the offset should be measured at 18.4 mm gap, where the taper is flat and the impedance of the taper itself is zero.

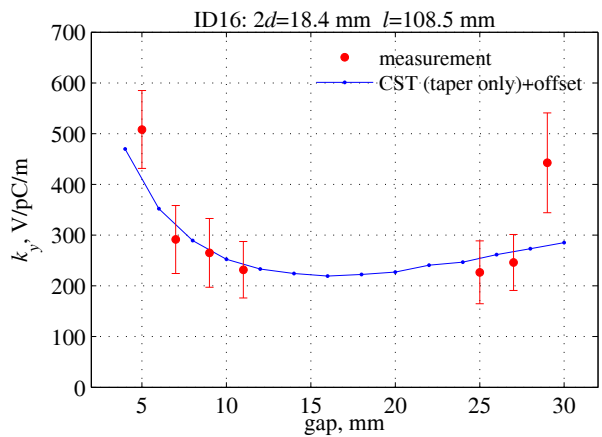


Figure 6: Vertical kick factor vs ID gap.

The gap-height dependence of the measured and simulated data looks quite consistent, except the point corresponding to the ID completely open (29 mm), where

the measurement conditions were different: $\Delta q = 0.9$ nC (10-bunch pattern) and $y_0 = 1$ mm, whereas for all other gap values measurements were performed with $\Delta q = 2 - 2.5$ nC (5-bunch pattern) and $y_0 = 1.5$ mm. So there are two possible reasons of the overestimated k_y value measured at 29 mm gap: either the measurement accuracy was poor because of smaller effect, which is proportional to $y_0\Delta q$, or the bunch-to-bunch interaction was not negligible because of smaller bunch-to-bunch distance.

Nevertheless, we can conclude that the BPM system of Diamond storage ring provides sufficient accuracy to measure such small effects.

REFERENCES

- [1] R. Bartolini, C.P. Bailey, M.P. Cox, N.P. Hammond, J. Kay, R.P. Walker, T. Pulampong, “Novel Lattice Upgrade Studies for Diamond Light Source”, IPAC’13, Shanghai, 2013, MOPEA068
- [2] <http://www.cst.com/Content/Products/PS/Overview.aspx>
- [3] V. Kiselev, V. Smaluk, “A Method for Measurement of Transverse Impedance Distribution along a Storage Ring”, DIPAC’99, Chester, 1999, PT19
- [4] V. Kiselev, V. Smaluk, NIM A 525, (2004) 433.
- [5] L. Emery, G. Decker, J. Galayda, “Bump Method for Measurement of Transverse Impedance of Narrow-Gap ID Chambers in Storage Rings”, PAC’01, Chicago, 2001, TPPH070
- [6] L. Tosi, E. Karantzoulis, V. Smaluk, “Measurements of the Impedance Introduced by the Vertical Scraper at ELETTRA and its Effects”, EPAC’02, Paris, 2002, WEPRI027